

Cyclopentadienyl/Alkoxo Ligand Exchange in Group 4 Metallocenes: A Convenient Route to Heterometallic Species

Piotr Sobota,^{*,†} Anna Drag-Jarząbek,[†] Łukasz John,[†] Józef Utko,[†] Lucjan B. Jerzykiewicz,[†] and Marek Duczmal[†]

[†]Faculty of Chemistry, University of Wrocław, ul. F. Joliot-Curie 14, 50-383 Wrocław, Poland, and ^{*}Faculty of Chemistry, Wrocław University of Technology, Wybrzeże Wyspiańskiego 27, 50-370 Wrocław, Poland

Received March 13, 2009

A simple and efficient strategy for the synthesis of nonorganometallic heterometallic clusters from cheap organometallic precursors is reported. This unique synthetic method involves elimination of the cyclopentadienyl ring from Cp₂MCl₂ (M = Ti, Zr, Hf) as CpH in the presence of M'L₂ or M'L'₂ (M' = Ca, Sr, Mn; CH₃OCH₂CH₂OH = LH or (CH₃)₂NCH₂CH₂OH = L'H) in an alcohol as a source of protons. In the reactions presented, a series of compounds, [Ca₄Ti₂(μ₆-O)(μ₃,η²-L)₈(η-L)₂Cl₄] (1), [Sr₄Hf₂(μ₆-O)(μ₃,η²-L)₈(η-L)₂(η-LH)₄Cl₄] (2), [Ca₄Zr₂(μ₆-O)(μ-Cl)₄(μ,η²-L)₈Cl₂] (3), [Sr₄Ti₂(μ₆-O)(μ₃,η²-L)₈(η-L)₂(η-LH)₂Cl₄] (4), [Ca₄Zr₂Cp₂(μ₄-Cl)(μ-Cl)₃(μ₃,η²-L)₄(μ,η²-L)₄Cl₂] (5), [CaTiCl₂(μ,η²-L')₃(η-L'H)₃][L'] (6), [Ca₂Ti(μ,η²-L')₆Cl₂] (7), [Mn₄Ti₄(μ-Cl)₂(μ₃,η²-L)₂(μ,η²-L)₁₀Cl₆] (8), and [Mn₁₀Zr₁₀(μ₄-O)₁₀(μ₃-O)₄(μ₃,η²-L)₂(μ,η²-L)₁₆(μ,η-L)₄(η-L)₂Cl₈] (9), were obtained in good yield. All of the complexes were characterized by elemental analysis, IR and NMR spectroscopy, and single-crystal X-ray structural analysis. Complex 8 belongs to a group of magnetic clusters that consists of Mn₄ subunits held together by two μ-Cl bridges. Compounds 6 and 7 underwent thermal decomposition, yielding an alternative source for some heterometallic oxides, which were analyzed by X-ray powder diffraction.

Introduction

In the area of inorganic chemistry, there is widespread interest in heterometallic complexes, especially those containing transition and main group metals.¹ Such species possess fascinating structural chemistry, interesting catalytic properties, and high potential for industrial applications.² The broad applicability of such compounds is a result of a cooperation between two different metals in a single molecule, which gives rise to properties that are not a simple sum of the properties of the individual metals and is often crucial for a system to achieve the desired activity. Thus, it is of interest to develop a new synthetic strategy to incorporate alkali metals into M-OR systems to generate compounds containing the M'-O(R)-M unit (M = transition metals, M' = main group metals). In this regard, the work of Bradley,^{3a,3b}

Mehrotra and Singh,^{3c} and Roesky et al.⁴ on the synthesis and the catalytic properties of alkoxo heterometallic complexes is notable. On the other hand, alkoxo complexes are perfect candidates for sol-gel and metal-organic chemical vapor-phase deposition conversion to corresponding oxide products.^{5a,5b} Furthermore, polymetallic clusters of paramagnetic metal ions have attracted much study since the discovery that such molecules can display single-molecule magnetism (SMM).⁶ Only very few studies have been undertaken to examine the magnetic properties of heterometallic clusters, even though SMM will lead to an understanding of quantum tunneling effects through synergy of metallic spins.⁷ These are crucial for today's technology and are utilized

*To whom correspondence should be addressed. Tel.: 048713757306. Fax: 048713282348. E-mail: plas@wchuw.pl.

(1) (a) Evans, W. J.; Ansari, M. A.; Ziller, J. W. *Polyhedron* 1997, 19, 3429–3434 and references therein. (b) Fischbach, A.; Herdtweck, E.; Anwender, R.; Eickerling, G.; Scherer, W. *Organometallics* 2003, 22, 499–509 and references therein. (c) Giesbrecht, G. R.; Gordon, J. C.; Brady, J. T.; Clark, D. L.; Keogh, D. W.; Michalczyk, R.; Scott, B. L.; Watkin, J. G. *Eur. J. Inorg. Chem.* 2002, 723–731.

(2) (a) Boffa, L. S.; Nowak, B. M. *Chem. Rev.* 2000, 100, 1479–1494. (b) Angermund, K.; Fink, G.; Jensen, V. R.; Kleinschmidt, R. *Chem. Rev.* 2000, 100, 1457–1470. (c) Fink, G.; Steinmetz, B.; Zechlin, J.; Przybyla, C.; Tesche, B. *Chem. Rev.* 2000, 100, 1377–1390.

(3) (a) Bradley, D. C. *Chem. Rev.* 1989, 89, 1317–1322. (b) Bradley, D. C. *Polyhedron* 1994, 13, 1111–1121. (c) Mehrotra, R. C.; Singh, A. *Chem. Soc. Rev.* 1996, 1–14.

(4) Chai, J.; Jancik, V.; Singh, S.; Zhu, H.; He, C.; Roesky, H. W.; Schmidt, H.-G.; Noltemeyer, M.; Hosmane, N. S. *J. Am. Chem. Soc.* 2005, 127, 7521–7528.

(5) (a) Bednorz, J. G.; Müller, K. A. *Angew. Chem., Int. Ed.* 1988, 27, 735–748. (b) Hubert-Pfalzgraf, L. G. *Appl. Organomet. Chem.* 1992, 6, 627–643. (c) Fernández-García, M.; Martínez-Arias, A.; Hanson, J. C.; Rodríguez, J. A. *Chem. Rev.* 2004, 104, 4063–4104. (d) Tian, L.; Lye, W. H.; Deivaraj, T. C.; Vittal, J. J. *Inorg. Chem.* 2006, 45, 8258–8263. (e) Labouthee, A.; Wongkasemjit, S.; Traversa, E.; Laine, R. M. *J. Eur. Ceram. Soc.* 2000, 20, 91–97. (f) Mathur, S.; Veith, M.; Ruegamer, T.; Hemmer, E.; Shen, H. *Chem. Mater.* 2004, 16, 1304–1312. (g) Mathur, S.; Shen, H.; Veith, M. *J. Am. Ceram. Soc.* 2006, 89, 2027–2033.

(6) Sessoli, R.; Gatteschi, D.; Caneschi, A.; Novak, M. A. *Nature* 1993, 365, 141–143.

(7) (a) Wernsdorfer, W.; Aliaga-Alcalde, N.; Hendrickson, D. N.; Christou, G. *Nature* 2002, 416, 406–409. (b) Bogani, L.; Wernsdorfer, W. *Nat. Mater.* 2008, 7, 179–186.

for the production of superconductors, microelectronic circuits, sensors, and ferroelectric materials and ceramic materials.^{5c–5g} In our research group, we have also synthesized several structurally interesting heterometallic alkoxo-organometallic compounds using reactions of metal alkoxides, which have a protonated hydroxyl group(s) in the alcohol molecule present in the metal coordination sphere, with organometallic compounds $M'R_3$ ($M' = \text{Al, Ga, In; R} = \text{Me, Et}$).^{8–10} These studies encouraged us to look for other organometallic species as substrates for the synthesis of new materials. Our studies on group 4 metallocenes showed that Cp_2MCl_2 ($M = \text{Ti, Zr, Hf}$) are attractive and cheap precursors to an extensive range of novel polymeric molecular and supramolecular materials.

Experimental Section

General. All reactions and operations were performed under an inert atmosphere of N_2 using standard Schlenk techniques. Reagents were purified by standard methods: toluene, distilled from Na; CH_2Cl_2 , distilled from P_2O_5 ; and hexanes, distilled from Na. Calcium (turnings, 99%), strontium (granule, 99%), manganese (powder, 99.99%), 2-methoxyethanol (anhydrous liquid, 99.8%), and N,N -dimethylethanolamine (anhydrous, 99.5 + %) were obtained from Aldrich and used without further purification unless stated otherwise. Bis(cyclopentadienyl)titanium dichloride (Cp_2TiCl_2 , powder, 97%), bis(cyclopentadienyl)zirconium dichloride dichloride (Cp_2ZrCl_2 , powder, 98 + %), and bis(cyclopentadienyl)hafnium dichloride (Cp_2HfCl_2 , powder, 98%) were obtained from Aldrich and used without further purification. Infrared spectra were recorded on a Perkin-Elmer 180 spectrophotometer in Nujol mulls. Electronic absorption spectra in solution were recorded on a CARY-50 UV–vis (Varian) spectrometer at a concentration of 5×10^{-2} M. The solvent (2-methoxyethanol) used in absorption was of spectroscopic grade and used as purchased (Sigma-Aldrich). NMR spectra were obtained on a BRUKER ESP 300E spectrometer. Gas chromatography/mass spectrometry (GC/MS) analyses were recorded on an HP 5890II (Hewlett-Packard) gas chromatograph with a mass detector. Microanalyses were conducted with an ARL Model 3410 + ICP spectrometer (Fisons Instruments) and a VarioEL III CHNS (in-house). Magnetic susceptibility studies of complex **8** were performed in a temperature range from 1.8 to 300 K in a field of 500 mT, and magnetizations of up to 5 T at 2.0 K were measured with a Quantum Design SQUID magnetometer. Diamagnetic corrections (-995×10^{-6} emu mol⁻¹) were calculated using Pascal's constants. The oxide products were characterized recording X-ray powder diffraction (XRD) patterns with a DRON-1 diffractometer using $\text{Cu K}\alpha$ radiation ($\lambda = 1.5418 \text{ \AA}$) filtered with Ni. The measurements were done for $2\theta = 10\text{--}90^\circ$ with a 2θ step = 0.1° .

[Ca₄Ti₂(μ_6 -O)(μ_3 , η^2 -L)₈(η -L)₂Cl₄] (1). Method A. A Schlenk flask was charged with Cp_2TiCl_2 (1.08 g; 4.34 mmol), metallic Ca (0.69 g; 17.22 mmol), 30 mL of LH (28.92 g; 0.38 mol), and

toluene $\text{C}_6\text{H}_5\text{CH}_3$ (30 mL). Stirring the dark-red solution resulted in a slow change of color to blue and then to light yellow over a period of 3 to 4 h. The mixture was vigorously stirred at room temperature until all of the metal was consumed (usually 4–5 h). After that time, the cloudy solution was filtered off. The filtrate was reduced under vacuum conditions to a powder. A total of 80 mL of hexanes were added, and the mixture was stirred for about 30 min. The precipitate was filtered off, washed with hexanes (3×15 mL), and dried to give **1** as a light-brown powder (1.82 g; 1.56 mmol, 72%). Colorless crystals of **1** were grown by layering hexanes over a toluene solution of **1**. Anal. calcd for $\text{C}_{30}\text{H}_{70}\text{O}_{21}\text{Cl}_4\text{Ti}_2\text{Ca}_4$ (MW, 1164.78): C, 30.94; H, 6.06; Cl, 12.18; Ca, 13.76; Ti, 8.22. Found: C, 30.74; H, 6.02; Cl, 12.23; Ca, 13.69; Ti, 8.24. IR (cm⁻¹, Nujol mull): 1820(w), 1640(w), 1460(vs), 1377(s), 1278(w), 1242(m), 1200(m), 1113(vs), 1060(vs), 1019(s), 966(w), 908(s), 837(s), 720(m), 676(s), 585(s), 460(s), 422(m), 386(m), 318(vw), 253(vw), 242(w). ¹H NMR (CDCl_3 , 298 K): δ 4.35–4.32 (t, 2H of CH_2), 3.73 (s, 3H of CH_3), 3.45–3.41 (t, 2H of CH_2). GC/MS: CpH (MW, 66), CpH dimer (traces), 1-methylcyclohexa-1,4-diene (traces), cyclopentene (traces). **Method B.** Complex **1** was also obtained during reaction of Cp_2TiCl_2 and CaL_2 (synthesis of calcium 2-methoxyethoxide was carried out according to the literature procedure: Goel, S. C.; Matchett, M. A.; Chiang, M. Y.; Buhro, W. E. *J. Am. Chem. Soc.* **1991**, *113*, 1844) using Cp_2TiCl_2 (0.85 g; 3.41 mmol), CaL_2 (1.30 g; 6.82 mmol), 5 mL of LH (4.82 g; 63.00 mmol), and toluene $\text{C}_6\text{H}_5\text{CH}_3$ (40 mL). A procedure analogous to that for method A gave colorless block crystals of **1** after 48 h. Elemental analysis and spectroscopic data confirmed that the obtained compound was complex **1**.

[Sr₄Hf₂(μ_6 -O)(μ_3 , η^2 -L)₈(η -L)₂(η -LH)₄Cl₄] (2). The procedure was the same as that described for **1** (method A or B) with Cp_2HfCl_2 and metallic Sr or SrL_2 instead of Cp_2TiCl_2 and metallic Ca or CaL_2 . Yield: 1.66 g; 0.86 mmol; 64%. Colorless block crystals of **2** were grown by layering hexanes over a toluene solution of **2**. Anal. calcd for $\text{C}_{42}\text{H}_{102}\text{O}_{29}\text{Cl}_4\text{Sr}_4\text{Hf}_2$ (MW, 1920.50): C, 26.27; H, 5.35; Cl, 7.38; Sr, 18.25. Found: C, 26.48; H, 5.26; Cl, 7.33; Sr, 18.27. IR (cm⁻¹, Nujol mull): 3410(w), 2753(w), 1637(w), 1458(vs), 1376(s), 1280(w), 1241(m), 1200(m), 1116(vs), 1056(vs), 1018(s), 967(w), 906(s), 839(s), 720(m), 677(s), 584(s), 461(s), 424(m), 386(m), 318(vw), 252(vw), 242(w). ¹H NMR (CDCl_3 , 298 K): δ 4.40 (br, 2H of CH_2), 3.71 (s, 3H of CH_3), 3.40 (br, 2H of CH_2). ¹³C{¹H} NMR (CDCl_3 , 298 K): δ 76.00 (s, CH_2), 68.32 (s, CH_2), 60.74 (s, CH_3). GC/MS: CpH (MW, 66), CpH dimer (traces), 1-methylcyclohexa-1,4-diene (traces), cyclopentene (traces).

[Ca₄Zr₂(μ_6 -O)(μ -Cl)₄(μ , η^2 -L)₈Cl₂]·2CH₂Cl₂ (3·2CH₂Cl₂). The procedure was the same as that described for **1** (method A or B) with Cp_2ZrCl_2 instead of Cp_2TiCl_2 . The filtrate was reduced under vacuum conditions to a powder and then dissolved in CH_2Cl_2 (60 mL). The solution was reduced under vacuum conditions to 20 mL. Colorless crystals of **3·2CH₂Cl₂** were obtained after several weeks (1.47 g; 1.09 mmol; 67%). Anal. calcd for $\text{C}_{26}\text{H}_{60}\text{O}_{17}\text{Cl}_{10}\text{Zr}_2\text{Ca}_4$ (MW, 1342.00): C, 23.27; H, 4.51; Cl, 26.42; Ca, 11.95; Zr, 13.59. Found: C, 22.98; H, 4.32; Cl, 25.86; Ca, 11.60; Zr, 13.15. IR (cm⁻¹, Nujol mull): 1460(vs), 1376(s), 1244(m), 1198(m), 1122(vs), 1074(vs), 1018(s), 914(m), 838(m), 780(vw), 722(vw), 662(m), 574(s), 464(s), 424(m), 404(m), 340(s), 240(m), 218(m). ¹H NMR (CDCl_3 , 298 K): δ 3.76–3.70 (m, 2H of CH_2), 3.50 (s, 3H of CH_3), 3.42–3.37 (m, 2H of CH_2). GC/MS: CpH (MW, 66), CpH dimer (traces).

[Sr₄Ti₂(μ_6 -O)(μ_3 , η^2 -L)₈(η -L)₂(η -LH)₂Cl₄] (4). The procedure was the same as that described for **1** (method A or B) with metallic Sr or SrL_2 instead of Ca or CaL_2 . Yield: 1.66 g; 1.23 mmol; 69%. Colorless block crystals of **4** were grown by layering hexanes over a toluene solution of **4**. Anal. calcd for $\text{C}_{36}\text{H}_{86}\text{O}_{25}\text{Cl}_4\text{Sr}_4\text{Ti}_2$ (MW, 1507.13): C, 28.69; H, 5.75; Cl,

(8) (a) John, L.; Utiko, J.; Szafert, S.; Jerzykiewicz, L. B.; Kepiński, L.; Sobota, P. *Chem. Mater.* **2008**, *20*, 4231–4239. (b) Szafert, S.; John, L.; Sobota, P. *Dalton Trans.* **2008**, 6509–6520.

(9) (a) Utiko, J.; Ejfler, J.; Szafert, S.; John, L.; Jerzykiewicz, L. B.; Sobota, P. *Inorg. Chem.* **2006**, *45*, 5302–5306. (b) Jerzykiewicz, L. B.; Utiko, J.; Sobota, P. *Organometallics* **2006**, *25*, 4924–4926. (c) Utiko, J.; Lizurek, A.; Jerzykiewicz, L. B.; Sobota, P. *Organometallics* **2004**, *23*, 296–298. (d) Utiko, J.; Przybylak, S.; Jerzykiewicz, L. B.; Szafert, S.; Sobota, P. *Chem. Eur. J.* **2003**, *9*, 181–190. (e) Sobota, P. *Coord. Chem. Rev.* **2004**, *248*, 1047–1060. (f) Sobota, P.; Utiko, J.; Sztajnowska, K.; Ejfler, J.; Jerzykiewicz, L. B. *Inorg. Chem.* **2000**, *39*, 235–239. (g) Utiko, J.; Szafert, S.; Jerzykiewicz, L. B.; Sobota, P. *Inorg. Chem.* **2005**, *44*, 5194–5196.

(10) Sobota, P.; Przybylak, K.; Utiko, J.; Jerzykiewicz, L. B.; Armando, J. L.; Pombeiro, A. J. B.; Faatima, M.; Guedes, C.; Szczegot, K. *Chem. Eur. J.* **2001**, *7*, 951–958.

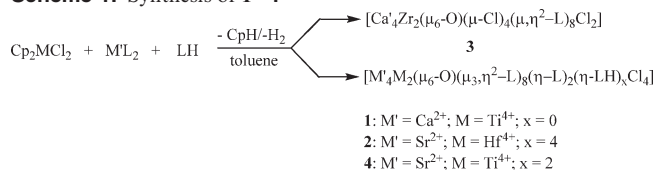
9.41; Sr, 23.26; Ti, 6.35. Found: C, 28.60; H, 5.66; Cl, 9.83; Sr, 23.27; Ti, 6.24. IR (cm^{-1} , Nujol mull): 3420 (w), 2720(w), 1636 (w), 1460 (vs), 1376 (s), 1282 (w), 1244 (m), 1196 (m), 1116 (vs), 1058 (vs), 1018 (s), 966 (w), 906 (s), 836 (s), 722 (m), 676 (s), 584 (s), 458 (s), 424 (m), 386 (m), 320 (vw), 252 (vw), 244 (w). ^1H NMR (CDCl_3 , 298 K): δ 4.42 (br, 2H of CH_2), 3.72 (s, 3H of CH_3), 3.43 (br, 2H of CH_2). $^{13}\text{C}\{^1\text{H}\}$ NMR (CDCl_3 , 298 K): δ 76.07 (s, CH_2), 68.32 (s, CH_2), 60.66 (s, CH_3). GC/MS: CpH (MW, 66), CpH dimer (traces), 1-methylcyclohexa-1,4-diene (traces), cyclopentene (traces).

[Ca₄Zr₂Cp₂(μ_4 -Cl)(μ -Cl)₃(μ_3 , η^2 -L)₄(μ , η^2 -L)₄Cl₂] \cdot 1.5CH₂Cl₂ (5**·1.5CH₂Cl₂). A Schlenk flask was charged with Cp₂ZrCl₂ (2.06 g; 7.05 mmol), CaL₂ (1.46 g; 9.23 mmol), 30 mL of LH (28.92 g; 0.38 mol), 30 mL of C₆H₅CH₃, and 40 mL of CH₂Cl₂. During the reaction, a white precipitate settled out. The mixture was stirred at room temperature for 12 h. After that time, the solution was filtered off. The precipitate was dried and dissolved in THF (60 mL) at 70 °C. The clear solution was reduced under vacuum conditions to 30 mL. Colorless crystals of **5**·1.5CH₂Cl₂ were obtained after 96 h (3.00 g; 2.33 mmol; 66%). Anal. calcd for C₇₁H₁₃₆O₃₂Cl₁₈Ca₈Zr₄ (MW, 2825.42): C, 30.18; H, 4.85; Cl, 22.59; Ca, 11.35; Zr, 12.91. Found: C, 29.90; H, 4.23; Cl, 21.83; Ca, 11.24; Zr, 12.54. IR (cm^{-1} , Nujol mull): 1831 (vw), 1457 (vs), 1377 (m), 1257 (w), 1242 (w), 1197 (m), 1097 (s), 1078 (s), 1061 (vs), 1014 (s), 960 (w), 893 (m), 841 (s), 760 (m), 597 (s), 499 (m), 435 (m), 429 (m), 418 (m), 305 (w), 277 (w), 254 (m). ^1H NMR (CDCl_3 , 298 K): δ 6.56–6.09 (m, 5H of Cp), 4.32–4.29 (t, 2H of CH_2), 3.70 (s, 3H of CH_3), 3.47–3.43 (m, 2H of CH_2). GC/MS: CpH (MW, 66), CpH dimer (traces), 1-methylcyclohexa-1,4-diene (traces), cyclopentene (traces).**

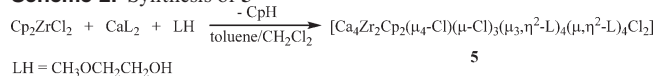
[CaTiCl₂(μ , η^2 -L)₃(η -L'H)₃][L'] (**6**). **Method A.** A Schlenk flask was charged with Cp₂TiCl₂ (0.9 g; 3.61 mmol), metallic Ca (0.15 g; 3.74 mmol), 20.00 mL of L'H (17.80 g; 0.20 mol), and toluene C₆H₅CH₃ (40 mL). The mixture was stirred at 80 °C for 2 h. After that time, all of the metal had been consumed. Stirring the dark-red solution resulted in a slow change of color to blue and then to light yellow. A light-brown precipitate settled out during the reaction. The solution was filtered off, and the precipitate was washed with toluene (2 \times 15 mL) and hexane (2 \times 15 mL) and then dried to give **6** as a white powder (1.66 g; 2.13 mmol; 59%). The filtrate was reduced under vacuum conditions to 20 mL; then hexane (10 mL) was added and formed a layer over the toluene solution. Colorless crystals of **6** were grown after 24 h. Anal. calcd for C₂₈H₇₃N₇O₇Cl₂CaTi (MW, 778.80): C, 43.18; H, 9.45; N, 12.59; Cl, 9.10; Ca, 5.15; Ti, 6.15. Found: C, 41.12; H, 9.55; N, 11.99; Cl, 9.36; Ca, 5.28; Ti, 6.11. IR (cm^{-1} , Nujol mull): 3312 (m), 2944 (vs), 1653 (vw), 1268 (m), 1181 (m), 1165 (m), 1090 (s), 1034 (s), 952 (m), 784 (m), 625 (m), 604 (m), 503 (m), 455 (m), 369 (w), 329 (vw), 222(w). ^1H NMR (CDCl_3 , 298K): δ 4.06 (s, 1H of OH), 3.63 (s, 2H of CH_2), 2.48 (s, 2H of CH_2), 2.27 (s, 3H of CH_3). GC/MS: CpH (MW, 66), CpH dimer (traces). **Method B.** Complex **6** was also obtained during the reaction of Cp₂TiCl₂ and CaL'₂, using Cp₂TiCl₂ (0.90 g; 3.61 mmol), CaL'₂ (0.78 g; 3.61 mmol), 5 mL of L'H (4.45 g; 50.00 mmol), and toluene C₆H₅CH₃ (40 mL). A procedure analogous to that for method A gave colorless crystals of **6** after 24 h. Elemental analysis and spectroscopic data confirmed that the obtained compound was complex **6**.

[Ca₂Ti(μ , η^2 -L)₆Cl₂] (**7**). **Method A.** A Schlenk flask was charged with Cp₂TiCl₂ (1.00 g; 4.02 mmol), metallic Ca (0.39 g; 9.73 mmol), 20 mL of L'H (17.80 g; 0.20 mol), and toluene C₆H₅CH₃ (20 mL). The mixture was stirred at 80 °C for 10 h. Stirring the dark-red solution resulted in a slow change of color to blue and then to light yellow over a period of 2 to 3 h. A light-brown precipitate settled out during the reaction. After that time, all of the metal had been consumed, and the solution was filtered off. The precipitate was washed with toluene (2 \times 15 mL) and hexane (2 \times 15 mL), then dried to give **7** as a white powder

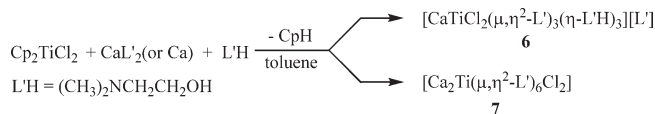
Scheme 1. Synthesis of 1–4



Scheme 2. Synthesis of 5



Scheme 3. Synthesis of 6 and 7



(2.05 g; 2.82 mmol; 70%). The filtrate was reduced under vacuum conditions to 20 mL; then hexane (20 mL) was added and formed a layer over the toluene solution. Colorless crystals of **7** were obtained after 24 h. Anal. calcd for C₂₄H₆₀N₆O₆Cl₂TiCa₂ (MW, 727.72): C, 39.61; H, 8.31; N, 11.55; Cl, 9.74; Ca, 11.02; Ti, 6.58. Found: C, 39.34; H, 8.77; N, 11.21; Cl, 9.86; Ca, 10.61; Ti, 5.97. IR (cm^{-1} , Nujol mull): 2924 (vs), 2775 (s), 2699 (m), 1422 (w), 1403 (vw), 1356 (s), 1278 (s), 1251 (m), 1185 (m), 1170 (w), 1082 (vs), 1066 (vs), 1036 (vs), 1027 (vs), 951 (vs), 889 (vs), 783 (s), 617 (w), 578 (vs), 500 (vs), 463 (vs), 437 (vs), 395 (vs), 335 (s), 283 (vs) 207 (s). ^1H NMR (CDCl_3 , 298 K): δ 3.59 (s, 2H of CH_2), 2.44 (s, 2H of CH_2), 2.25 (s, 3H of CH_3). GC/MS: CpH (MW, 66), CpH dimer (traces). **Method B.** Complex **6** was also obtained during the reaction of Cp₂TiCl₂ and CaL'₂ using Cp₂TiCl₂ (1.00 g; 4.02 mmol), CaL'₂ (1.74 g; 8.04 mmol), 5 mL of L'H (4.45 g; 50.00 mmol), and toluene C₆H₅CH₃ (40 mL). An analogous procedure to method A gave after 24 h colorless crystals of **7**. Elemental analysis and spectroscopic data confirmed the nature of complex **7**.

[Mn₄Ti₄(μ -Cl)₂(μ_3 , η^2 -L)₂(μ , η^2 -L)₁₀Cl₆] \cdot 2C₆H₅CH₃ (8**·2C₆H₅CH₃). A Schlenk flask was charged with Cp₂TiCl₂ (1.29 g; 5.2 mmol), metallic Mn (1.32 g; 24 mmol; Ti : M_n = 1 : 4.6), 30 mL of LH (28.92 g; 0.38 mol), and toluene C₆H₅CH₃ (20 mL). The mixture was stirred at 80 °C for 12 h. After that time, the solution was filtered off. The filtrate was reduced under vacuum conditions to 30 mL. Green column crystals of **8**·2C₆H₅CH₃ were obtained from the toluene solution after 96 h (1.43 g; 0.80 mmol; 62%). Anal. calcd for C₅₀H₁₀₀O₂₄Cl₈Mn₄Ti₄·2C₆H₅ (MW, 1780.26): C, 33.73; H, 5.66; Cl, 15.93; Ti, 10.76; Mn, 12.34. Found: C, 33.60; H, 5.63; Cl, 15.83; Ti, 10.57; Mn, 12.24. IR (cm^{-1} , Nujol mull): 1828 (vw), 1460 (vs), 1376 (m), 1260 (w), 1240 (w), 1194 (m), 1096 (s), 1078 (s), 1056 (vs), 1016 (s), 964 (w), 894 (m), 836 (s), 762 (m), 596 (s), 500 (m), 432 (m), 428 (m), 420 (m), 304 (w), 276 (w), 252 (m). UV–Vis: 576 nm. GC/MS: CpH (MW, 66), CpH dimer (traces), 1-methylcyclohexa-1,4-diene (traces), cyclopentene (traces).**

[Mn₁₀Zr₁₀(μ_4 -O)₁₀(μ_3 -O)₄(μ_3 , η^2 -L)₂(μ , η^2 -L)₁₆(μ , η -L)₄(η -L)₂-Cl₈] (**9**). A Schlenk flask was charged with Cp₂ZrCl₂ (3.02 g; 10.33 mmol), metallic Mn (1.50 g; 27.30 mmol), 50 mL of LH (48.20 g; 0.63 mol), and toluene (30 mL). The mixture was stirred at 80 °C for 12 h. After that time, the solution was filtered off. The filtrate was reduced under vacuum conditions to 30 mL. Colorless crystals of **9** were obtained after 96 h (2.41 g; 0.64 mmol; 62%). Anal. calcd for C₇₂H₁₆₈O₆₂Cl₈Mn₁₀Zr₁₀ (MW, 3771.26): C, 22.93; H, 4.49; Cl, 7.52; Mn, 14.57; Zr, 24.19. Found: C, 22.13; H, 4.17; Cl, 7.38; Mn, 14.06; Zr, 24.04. IR (cm^{-1} , Nujol mull): 1727 (w), 1600 (vw), 1496 (m), 1277 (m), 1245 (m), 1200 (m), 1180 (vs), 1102 (vs), 1051 (vs), 1016 (vs), 914 (vs), 842 (s), 736 (vs),

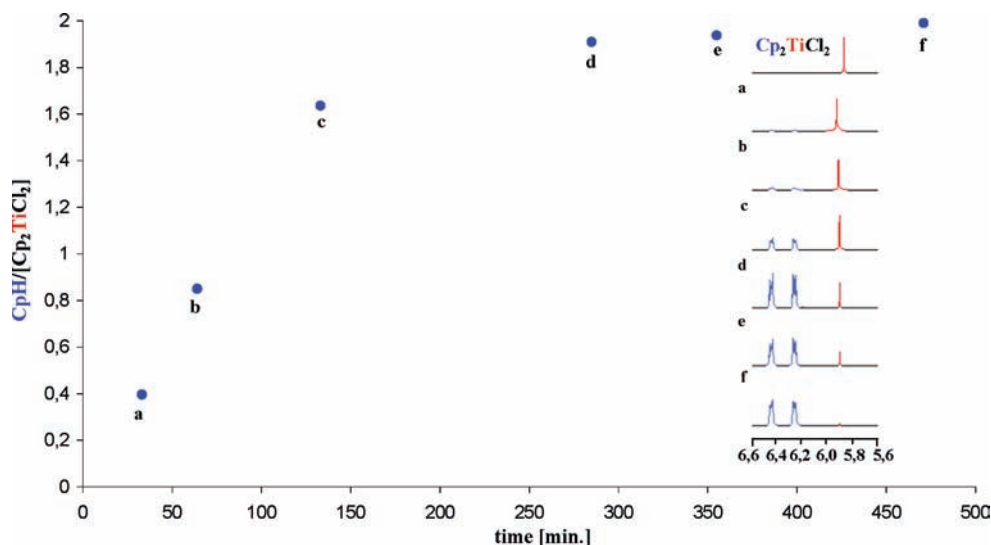
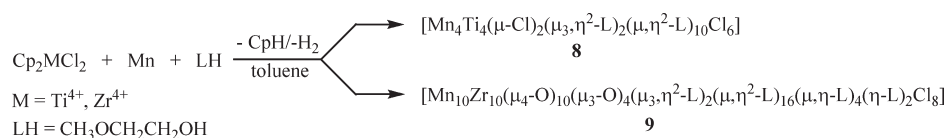


Figure 1. ^1H NMR CpH spectra as a plot of the CpH/Cp₂TiCl₂ ratio against time for the reaction of Cp₂TiCl₂ with CaL'₂ and L'H (1: 2: 6) in toluene-*d*₈.

Scheme 4. Synthesis of **8** and **9**



698 (vs), 625 (vs), 574 (s), 530 (m), 511 (m), 461 (w), 401 (vw), 339 (m), 258 (m), 241 (m). GC/MS: CpH (MW, 66), CpH dimer (traces), 1-methylcyclohexa-1,4-diene (traces), cyclopentene (traces).

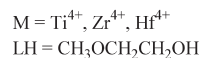
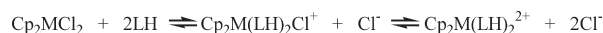
Results and Discussion

Synthesis. Reaction of Cp₂MCl₂ (M = Ti, Zr, Hf) with 2 equiv of M'L₂ (M' = Ca, Sr) and an excess of LH (LH = 2-methoxyethanol) in toluene at room temperature gave the colorless cyclopentadienyl-free heterometallic compounds [Ca₄Ti₂(μ₆-O)(μ₃,η²-L)₈(η-L)₂Cl₄] (**1**), [Sr₄Hf₂(μ₆-O)(μ₃,η²-L)₈(η-L)₂(η-LH)₄Cl₄] (**2**), [Ca₄Zr₂(μ₆-O)(μ-Cl)₄(μ,η²-L)₈Cl₂] (**3**), and [Sr₄Ti₂(μ₆-O)(μ₃,η²-L)₈(η-L)₂(η-LH)₂Cl₄] (**4**) after 12 h in good yield (Scheme 1).

The mild reactivity of the cyclopentadienyl/alkoxo ligand exchange makes it possible to isolate some of the intermediates and sheds light on the reaction pathway. When the reaction of Cp₂ZrCl₂ with CaL₂ in the presence of LH was carried out in toluene/CH₂Cl₂ for 6 h, the intermediate [Ca₄Zr₂Cp₂(μ₄-Cl)(μ-Cl)₃(μ₃,η²-L)₄(μ,η²-L)₄Cl₂] (**5**) was isolated (Scheme 2). Methane dichloride was added to decrease the solubility of the resulting products. To simplify the reactions, metallic M' can be added instead of M'L₂ directly to Cp₂MCl₂ in a toluene/LH solution. In this case, M'L₂ is formed in situ directly from M' and LH. Moreover, the reaction pathway and the composition of the final products may be controlled by means of the M'/Cp₂MCl₂ ratio and the kind of alcohol. The reaction of Cp₂TiCl₂ with 1 or 2 equiv of CaL'₂ in N,N-dimethylethanolamine (L'H) causes the formation of the complexes [CaTiCl₂(μ,η²-L')₃(η-L')₃][L'] (**6**) and [Ca₂Ti(μ,η²-L')₆Cl₂] (**7**), respectively (Scheme 3).

In the meantime, we were also interested in exploring the reaction of group 4 metallocenes with manganese, which has interesting magnetic properties. When Cp₂TiCl₂

Scheme 5. The Chloride Dissociation Equilibrium of Cp₂MCl₂ in LH



reacts with an excess of metallic Mn in toluene/LH at 80 °C, a green solution is formed, from which cyclopentadienyl-free paramagnetic blue crystalline [Mn₄Ti₄(μ-Cl)₂(μ₃,η²-L)₂(μ,η²-L)₁₀Cl₆] (**8**) precipitates. Furthermore, the addition of metallic manganese to Cp₂ZrCl₂ in toluene/LH results in the formation of a Cp-free heterometallic cluster with the formula [Mn₁₀Zr₁₀(μ₄-O)₁₀(μ₃-O)₄(μ₃,η²-L)₂(μ,η²-L)₁₆(μ,η-L)₄(η-L)₂Cl₈] (**9**) (Scheme 4). The excess of manganese, which accelerates the reaction, is easily removed by filtration, and the complexes can be crystallized out almost quantitatively from the filtrate.

The appearance of free cyclopentadiene during the reaction of Cp₂TiCl₂ with CaL'₂ in toluene-*d*₈/L'H was monitored using the ^1H NMR technique and recorded at various time intervals, generally up to 12 h, with the sample maintained at room temperature. The recorded CpH spectra make it possible to plot the dependence of CpH/Cp₂TiCl₂ as a function of time (Figure 1). For Cp₂TiCl₂, the amount of loss of titanium-bound Cp was calculated by integrating the liberated CpH at δ 6.42–6.48 ppm (2H of CpH) resonances versus the remaining metal-bound η⁵-Cp signals at δ 5.92–5.94 ppm. The half-life of ring loss for the Cp₂TiCl₂/CaL'₂/L'H reaction is ca. 1.0 h, and the chemical shifts of the remaining rings are shifted toward lower frequencies compared with Cp₂TiCl₂ in toluene-*d*₈ at δ 5.89 ppm and are not equivalent (Scheme 5 and Figure S9, Supporting Information). The conversion was complete within 8 h, as evidenced by

Table 1. Crystallographic Data for 1–5 and 7–9

compound	1	2	3	4
empirical formula	C ₃₀ H ₇₀ Ca ₄ Cl ₄ O ₂₁ Ti ₂	C ₄₂ H ₁₀₂ Cl ₄ Hf ₂ O ₂₉ Sr ₄	C ₂₆ H ₆₀ Ca ₄ Cl ₁₀ O ₁₇ Zr ₂	C ₃₆ H ₈₆ Cl ₄ O ₂₅ Sr ₄ Ti ₂
<i>M</i>	1164.78	1920.50	1342.00	1507.13
cryst syst	triclinic	triclinic	triclinic	monoclinic
space group	<i>P</i> $\bar{1}$	<i>P</i> $\bar{1}$	<i>P</i> $\bar{1}$	<i>P</i> 2 ₁ / <i>n</i>
<i>a</i> (Å)	10.716(4)	12.184(4)	11.019(5)	12.167(4)
<i>b</i> (Å)	11.923(5)	12.833(4)	11.808(5)	12.635(4)
<i>c</i> (Å)	12.384(5)	13.258(5)	11.829(6)	19.566(5)
α (deg)	107.03(1)	64.54(3)	104.15(4)	90
β (deg)	115.23(1)	75.31(2)	115.31(5)	94.15(2)
γ (deg)	102.48(1)	66.39(3)	92.92(4)	90
<i>V</i> (Å ³)	1257.8(9)	1706.7(10)	1327.8(13)	3000.0(16)
<i>Z</i>	1	1	1	2
<i>D</i> _{calcd} (mg/m ³)	1.538	1.865	1.678	1.668
cryst size (mm ³)	0.283 × 0.148 × 0.087	0.244 × 0.197 × 0.113	0.212 × 0.182 × 0.036	0.44 × 0.20 × 0.13
μ (mm ⁻¹)	1.007	6.363	1.338	4.034
θ (deg)	2.86 to 28.00	2.96 to 27.05	2.93 to 26.09	2.60 to 29.11
reflns collected	18313	20203	10492	40705
unique reflns, <i>R</i> _(int)	6028, 0.0239	7477, 0.0374	5230, 0.0189	8011, 0.1082
final <i>R</i> ₁ , <i>wR</i> ₂ [<i>I</i> > 2 σ (<i>I</i>)]	0.0269, 0.0718	0.0237, 0.0504	0.0281, 0.0742	0.0466, 0.0770
final <i>R</i> ₁ , <i>wR</i> ₂ (all data)	0.0340, 0.0740	0.0307, 0.0534	0.0353, 0.0773	0.1053, 0.0938
goodness-of-fit (<i>S</i>)	1.059	1.053	1.067	0.964

compound	5	7	8	9
empirical formula	C ₇₁ H ₁₃₆ Ca ₈ Cl ₁₈ O ₃₂ Zr ₄	C ₂₄ H ₆₀ Ca ₂ Cl ₂ N ₆ O ₆ Ti	C ₅₀ H ₁₀₀ Cl ₈ Mn ₄ O ₂₄ Ti ₄	C ₇₂ H ₁₆₈ Cl ₈ Mn ₁₀ O ₆₂ Zr ₁₀
<i>M</i>	2825.42	727.74	1780.26	3771.26
cryst syst	monoclinic	tetragonal	triclinic	triclinic
space group	<i>C</i> 2/ <i>c</i>	<i>P</i> 4 ₂ / <i>n</i>	<i>P</i> $\bar{1}$	<i>P</i> $\bar{1}$
<i>a</i> (Å)	31.259(7)	19.723(6)	10.700(5)	14.285(4)
<i>b</i> (Å)	17.216(5)	19.723(6)	10.787(6)	15.639(5)
<i>c</i> (Å)	23.455(6)	9.562(4)	18.960(6)	17.235(6)
α (deg)	90	90	85.12(3)	116.46(3)
β (deg)	111.19(4)	90	74.68(3)	94.63(2)
γ (deg)	90	90	77.63(3)	100.02(3)
<i>V</i> (Å ³)	11769(5)	3720(2)	2060.7(16)	3339(2)
<i>Z</i>	4	4	1	1
<i>D</i> _{calcd} (mg/m ³)	1.595	1.300	1.435	1.867
cryst size (mm ³)	0.132 × 0.082 × 0.074	0.212 × 0.193 × 0.082	0.212 × 0.101 × 0.092	0.211 × 0.182 × 0.112
μ (mm ⁻¹)	1.167	0.691	1.279	1.894
θ (°)	2.73 to 28.00	2.92 to 25.00	2.91 to 27.50	2.65 to 27.50
reflns collected	49331	8658	28065	48332
unique reflns, <i>R</i> _(int)	14064, 0.1334	3252, 0.0612	9425, 0.0687	15322, 0.1086
final <i>R</i> ₁ , <i>wR</i> ₂ [<i>I</i> > 2 σ (<i>I</i>)]	0.0581, 0.0894	0.0501, 0.1093	0.0390, 0.0745	0.0518, 0.0905
final <i>R</i> ₁ , <i>wR</i> ₂ (all data)	0.1720, 0.1194	0.0999, 0.1266	0.0880, 0.0845	0.1280, 0.1091
goodness-of-fit (<i>S</i>)	0.837	1.089	0.860	0.852

¹H NMR. Whether only one or both Cp ligands are exchanged or whether both processes take place side by side strongly depends upon the reactants involved, their stoichiometric ratio, the nature of the alcohol, and to a great extent the nature of the metals, M and M'. It is worth noting that the half-life of ring loss for Cp₂TiCl₂ in KNO₃/D₂O solution is 57.0 ± 0.9 h at 37 °C.¹¹ The dissolution of titanocene dichloride in water produces a low pH, in which the chloride ligands are replaced by H₂O and OH⁻ ligands, and results in protonation and loss of the Cp groups and the formation of insoluble Ti oxo species. It was also discovered that the addition of NEt₃ to the ethanol solution of Cp₂ZrCl₂ accelerates the hydrolysis process and shifts the chloride dissociation equilibria substantially to the right, and Zr(OEt)₄ is formed in good yield.¹²

On the basis of the facts discussed above, it is obvious that, in the first step, Cp₂MCl₂ undergoes transformation involving chloride loss and the coordination of LH to the

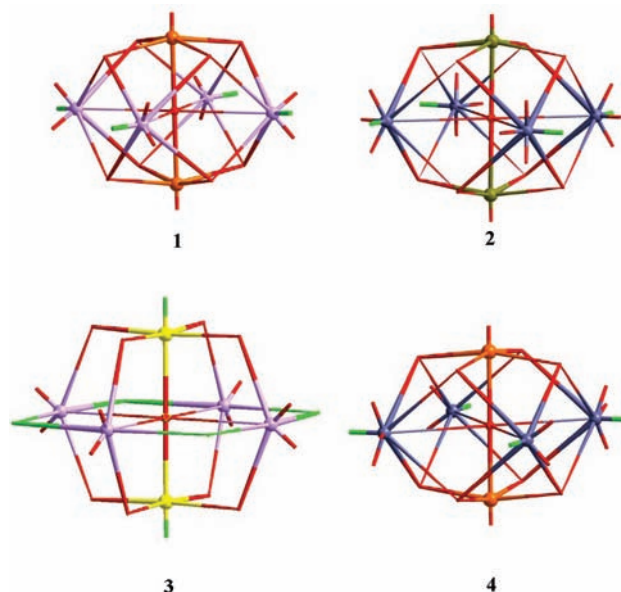


Figure 2. View of the octahedral cores in compounds 1–4.

(11) Toney, J. H.; Marks, T. J. *J. Am. Chem. Soc.* **1985**, *107*, 947–953.(12) Gray, D. R.; Brubaker, C. H. Jr. *Inorg. Chem.* **1971**, *10*, 2143–2146.

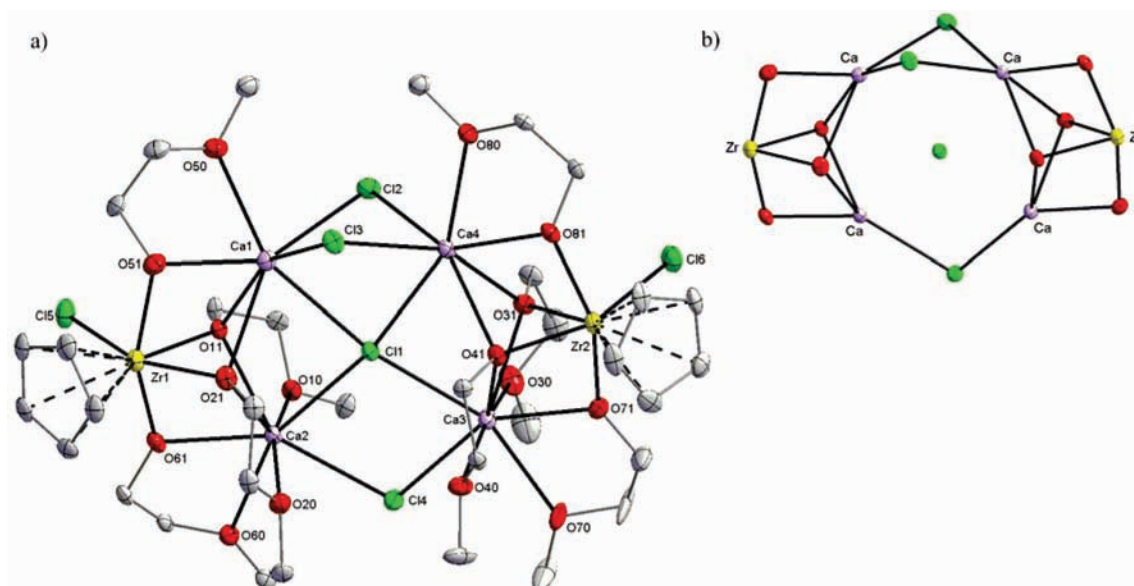


Figure 3. (a) Molecular structure of **5**. Hydrogen atoms omitted for clarity. (b) μ_4 -Cl in a $[\text{Ca}_4\text{Zr}_2(\mu\text{-Cl})_3(\mu_3\text{-O}_{\text{alkoxo}})_4(\mu\text{-O}_{\text{alkoxo}})_4]$ cage.

metal center, followed by partial or total replacement of the Cp groups by LH, providing in return proton functionalities necessary for CpH liberation (Scheme 5).¹³ In the second step, $\text{M}'\text{L}_2$ binds the Cl^- ions, shifts the chloride dissociation equilibria to the right, and accelerates a multiple-step process that proceeds with intermolecular elimination of CpH from the metal site and leads to the formation of compounds **1–9**. Compounds **1–9** were isolated as crystalline and thermally stable solids, air- and moisture-sensitive, and soluble in toluene at room temperature. In the IR spectra of **2**, **4**, and **6**, a broad absorption band near 3400 cm^{-1} is assigned to the stretching frequency of the coordinated alcohol hydroxide group.

X-Ray Structural Analyses. Crystals of complexes **1–9** were investigated using the single-crystal X-ray technique (Table 1). Selected structures of **1**, **5**, **7**, **8**, and **9** are shown in Figures 2, 3, 5–7, whereas all of the structures and structural fits of all compounds are depicted in the Supporting Information. The crystal structures of **1**, **2**, and **4** are based on hexanuclear entities of the general formula $[\text{M}_4\text{M}'_2(\mu_6\text{-O}_{\text{oxo}})(\mu_3\text{-O}_{\text{alkoxide}})_8]$ ($\text{M} = \text{Ca}, \text{Sr}$; $\text{M}' = \text{Ti}, \text{Hf}$). The metallic units can be described in two ways: first, as an octahedron with six metal centers and a μ_6 -oxo encapsulated oxygen atom residing at the central position and each of the triangular faces being capped by a μ_3 -oxygen atom of the alkoxide group (Figure 2); second, as a cube formed by the eight oxygen atoms of the alkoxide groups, with metal ions protruding out of the six faces of the cube and an oxo ion occupying the central position (Figure 2). In contrast to **1**, **2**, and **4**, compound **3** has a $[\text{Ca}_4\text{Zr}_2(\mu_6\text{-O})(\mu_2\text{-Cl})_4(\mu_2\text{-O}_{\text{alkoxo}})_8]$ octahedral core in which each edge of the polyhedron is alternately capped by $\mu_2\text{-O}_{\text{alkoxide}}$ groups or $\mu_2\text{-Cl}$ anions (Figure 2). In all hexanuclear complexes, the central μ_6 -oxo ion lies on an inversion center. The equatorial metal centers are six-coordinated in **3**, eight-coordinated in **1** and **4**,

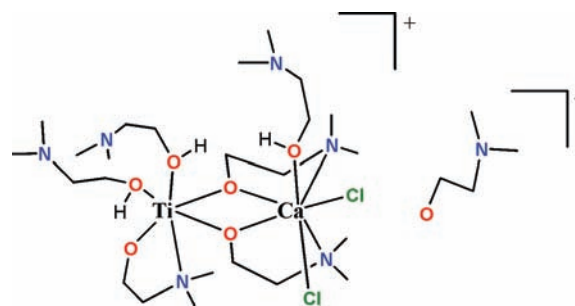


Figure 4. Drawing of **6**. Crystal data: monoclinic, $P2_1/n$, $a = 13.285(5)$, $b = 15.846(5)$, $c = 22.013(8)$ Å, $\beta = 117.48^\circ$, $T = 100$ K.

and nine-coordinated in **2**, whereas the axial metal ions are always six-coordinated. It was observed that, as the metal coordination number increased, so did the length of the $(\mu_6\text{-O}_{\text{oxo}})$ bond distances and the deformation of the octahedral entities. In all of these structures, the cores are slightly compressed in the axial direction with respect to the equatorial plane. Although the mechanism of $\mu_6\text{-O}$ oxo ligand formation is unknown, the most probable source of the O^{2-} anion is adventitious hydrolysis or alkene/ether elimination reactions.¹⁴ Furthermore, it is well-known that titanoxanes containing oxo-bridged linkages $\text{Ti}-\text{O}-\text{Ti}$, for example, in $[\text{Ti}_2(\mu\text{-O})\text{Cl}_2(\eta^2\text{-guaicolato})_4]$ or $[\text{Ti}_4(\mu\text{-O})_4\text{Cl}_8(\text{MeCN})_8]$, are formed in situ by controlled hydrolysis of titanium species.^{10,15}

The molecular structure of **5** showed a Ca_4 calcium center with two $[\text{Ca}_2\text{ZrCp}(\mu, \eta^2\text{-L})_4\text{Cl}_3]$ units joined by three $\mu\text{-Cl}$ bridging chloride atoms to form the $[\text{Ca}_4\text{Zr}_2\text{Cp}_2(\mu\text{-Cl})_3(\mu_3, \eta^2\text{-L})_4(\mu, \eta^2\text{-L})_4\text{Cl}_2]^+$ cation encapsulating the $\mu_4\text{-Cl}$ chloride ion in the center of the array (Figure 3). While a few examples of a $\mu_4\text{-Cl}$ bridging chloride ion on late metal complexes of Cu, Cd, Ag, and

(13) Sobota, P.; Utko, J.; John, Ł.; Jerzykiewicz, L. B.; Drąg-Jarząbek, A. *Inorg. Chem.* **2008**, *47*, 7939–7941.

(14) Turova, N. Yu.; Turevskaya, E. P.; Kessler, V. G.; Yanovsky, A. I.; Struchkov, Y. T. *J. Chem. Soc., Chem. Commun.* **1993**, 21.

(15) Willey, G. R.; Palin, J.; Drew, M. G. B. *J. Chem. Soc., Dalton Trans.* **1994**, 1799–1804 and references therein.

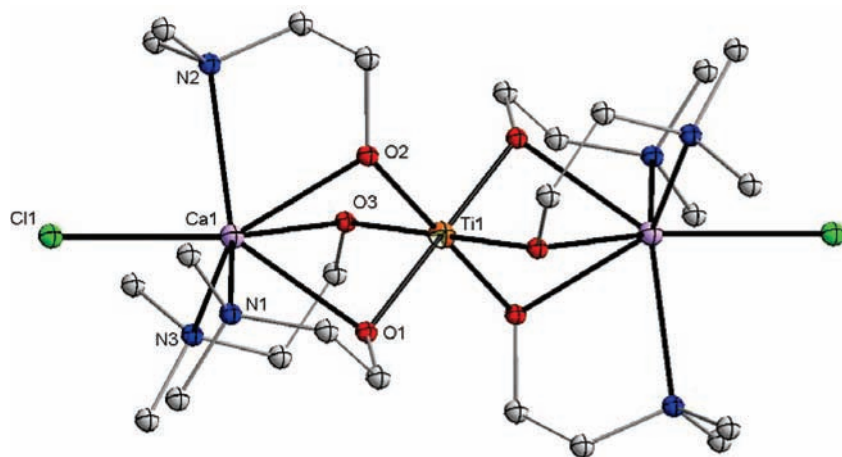


Figure 5. Molecular structure of 7. Hydrogen atoms omitted for clarity.

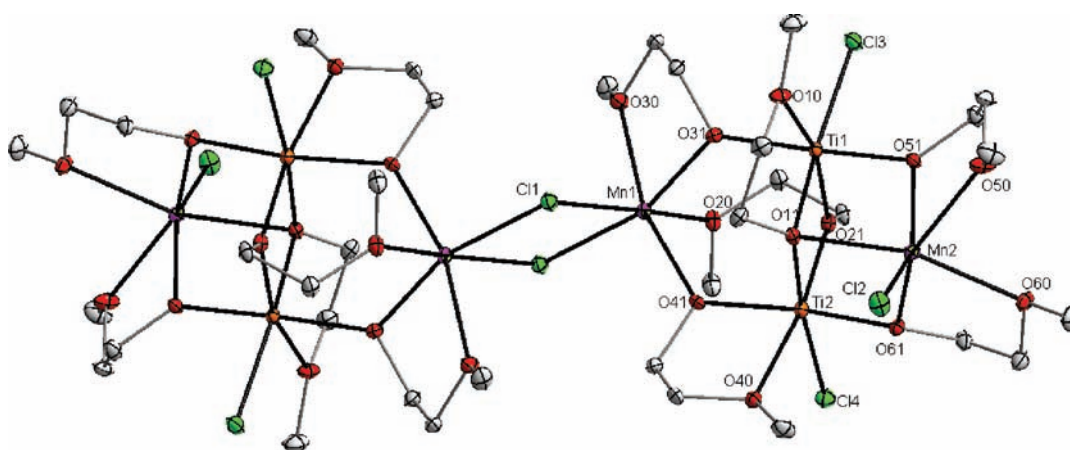


Figure 6. Molecular structure of 8. Hydrogen atoms omitted for clarity.

Hg have been reported,¹⁶ this is to the best of our knowledge the first unique example of a chloride μ_4 -Cl ion located in a Ca_4 cage.

Compound **6** was obtained in crystalline form and identified by elemental analysis, spectroscopic data, and X-ray diffraction studies. Unfortunately, its structure could not be determined completely due to low-quality crystals. Nonetheless, the structure is clearly visible and can be discussed. The dimeric $[\text{CaTiCl}_2(\mu, \eta^2\text{-L}')_3(\eta\text{-L}'\text{H})_3]^+$ cation is composed of $\text{Ca}(\eta^2\text{-L}')_2(\eta\text{-L}'\text{H})\text{Cl}_2$ and $\text{Ti}(\eta^2\text{-L}')(\text{L}'\text{H})_2$ moieties bridged by two amino-alkoxide oxygen atoms of the calcium L' ligands. The anion consists of deprotonated amino alcohol. An overall view of the molecule is presented in Figure 4. Complex **7** is composed of two calcium and one titanium ion that all, with terminal chloride atoms, lie in a straight line. The central Ti atom is located on an inversion center, and its coordination sphere consists of the six alkoxide atoms of the L' anions. The centrosymmetrically related terminal calcium atoms are seven-coordinated with $\text{N}_3\text{O}_3\text{Cl}$ donors (Figure 5).

The titanium–manganese compound **8** was obtained as blue crystals and characterized by X-ray structural analysis. The structural investigation reveals a centrosymmetric octanuclear dimer with an inversion center located at the midpoint of the central Mn_2Cl_2 fragment. It consists of two equivalent asymmetric $[\text{Mn}_2\text{Ti}_2(\mu\text{-Cl})-(\mu_3, \eta^2\text{-L})_2(\mu, \eta^2\text{-L})_{10}\text{Cl}_3]$ (**8**) moieties linked by two $\mu\text{-Cl}$ bridges (Figure 6). Each Mn_2Ti_2 unit can be described as two MnTi_2 triangular faces held together by the μ_3 - and μ_2 -oxygen atoms of the L ligands. The edges of each triangular face consist of μ_2 -oxygen atoms. The intermolecular $\text{Ti}\cdots\text{Ti}$ distance is 2.967(2) Å, which is comparable with the $\text{Ti}\cdots\text{Ti}$ distance in $\alpha\text{-Ti}$ metal (2.8956 Å).¹⁷ The intermolecular $\text{Mn}\cdots\text{Ti}$ distances range from 3.315(2) to 3.707(2) Å.

The zirconium–manganese structure of **9** consists of a $\text{Zr}_{10}\text{Mn}_{10}$ core held together by oxo, alkoxo, and chloride ligands with different coordination modes: μ_3 , μ_4 , μ_3, η^2 , μ, η^2 , μ, η , η , and μ (Figure 7). The whole complex can be divided into two guest–host subunits. The external, host unit (fuchsia) consists of 10 Mn^{2+} outer-perimeter ions linked with zirconium atoms by O_{oxo} and O_{alkoxo} . The internal, guest zirconium moiety (yellow) is formed

(16) (a) Müller, J. F. K.; Neuburger, M.; Weber, H.-P. *J. Am. Chem. Soc.* **1999**, *121*, 12212–12213. (b) Liaw, B.-J.; Lobana, T. S.; Lin, Y.-W.; Wang, J.-C.; Liu, C. W. *Inorg. Chem.* **2005**, *44*, 9921–9929. (c) Salta, J.; Zubieta, J. *Inorg. Chim. Acta* **1996**, *252*, 435–438. (d) Yang, X.; Knobler, C. B.; Zheng, Z.; Hawthorne, M. F. *J. Am. Chem. Soc.* **1994**, *116*, 7142–7159.

(17) Weast, R. C. *Handbook of Chemistry and Physics*, 57th ed.; CRC: Cleveland, OH, 1976; pp F–216.

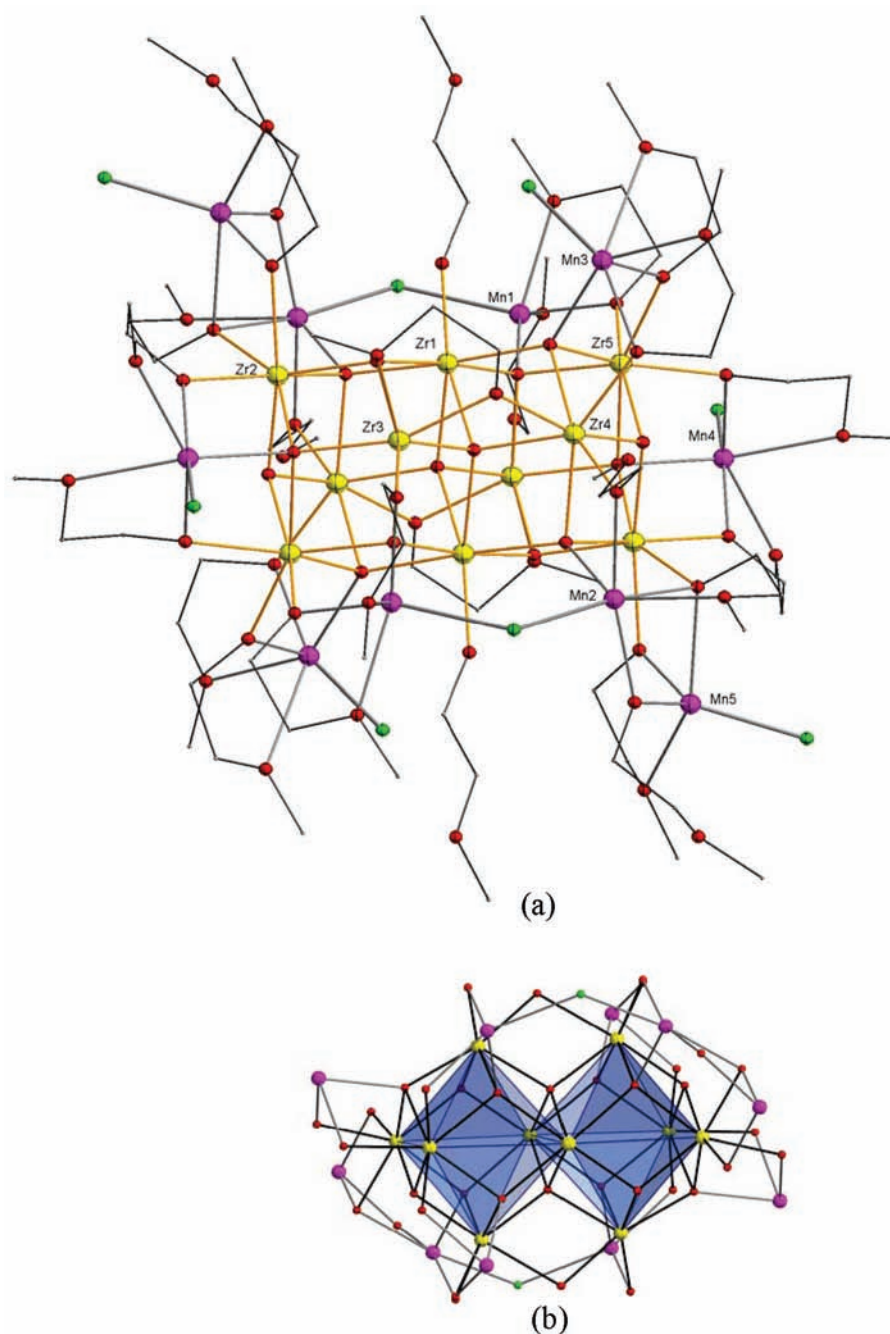
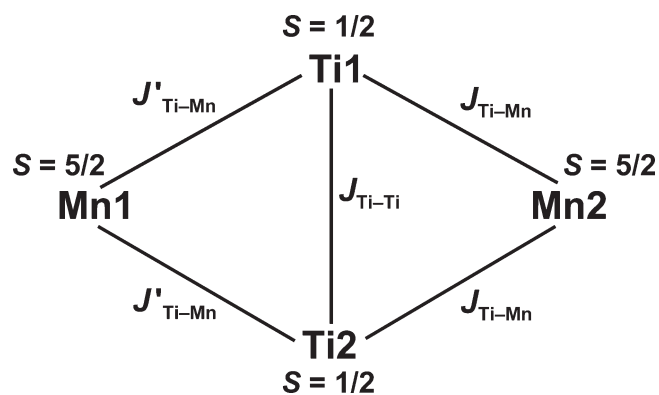


Figure 7. (a) Structure of **9**. Hydrogen atoms omitted for clarity. (b) Metal–oxygen core.

by two fused corner-shared Zr_6O_8 units, in which six zirconium ions are arranged at the apexes of an octahedron. The equatorial zirconium centers of fused octahedrons are in one plane. In contrast to the structures of **1**, **2**, and **4**, complex **9** does not have a μ_6 -O encapsulated oxygen atom inside the metallic core. Each fused Zr_6O_8 unit is also linked to others by two μ - $O_{alkoxide}$ atoms, in such a way that adamantane skeletons can be identified. The dodecanuclear zirconium core is surrounded by 10 manganese ions, which are joined to the metallic center by alkoxide and oxo oxygen atoms. The outer manganese unit is also stabilized by bridging chloride ions. All zirconium centers are seven-coordinated, whereas manganese ions are five- and six-coordinated.

Scheme 6. Possible Mn–Ti Magnetic Interactions



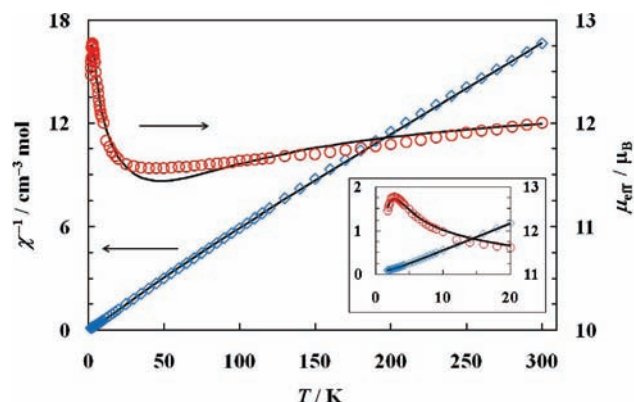


Figure 8. Variation of χ^{-1} (diamonds) and μ_{eff} (triangles) per $\text{Mn}^{\text{II}}_4\text{Ti}^{\text{III}}_4$ octamer with the temperature. The solid lines represent the fit to the Kambe model (see text for details).

Magnetic Properties of 8. The presented synthetic strategy can easily be envisioned as a convenient route to the synthesis of paramagnetic complexes which might have potential as SMMs. There are a number of articles and reviews that cover the broad range of $[\text{Mn}]_4$ chemistry from synthetic strategies to theoretical investigations.¹⁸ In contrast, fewer studies have been undertaken to examine the magnetic properties of heterometallic systems.¹⁹ The magnetic susceptibility of **8** (Figure 8) shows Curie–Weiss behavior in the temperature range 160–300 K, with the Weiss constant $\Theta = -18.3$ K and a magnetic moment of $12.34 \mu_{\text{B}}$, which is almost equal to the $12.33 \mu_{\text{B}}$ ($g = 2.00$) value expected for an uncoupled $\text{Mn}^{\text{II}}_4\text{Ti}^{\text{III}}_4$ core with local spins $S_{\text{Mn}} = 5/2$ and $S_{\text{Ti}} = 1/2$. The effective magnetic moment slowly decreases from $12.0 \mu_{\text{B}}$ at 300 K to a broad minimum of $11.6 \mu_{\text{B}}$ at 45 K. Below 45 K, the value increases and reaches a maximum of $12.78 \mu_{\text{B}}$ at 2.7 K, very close to the value expected for two isolated $\text{Mn}^{\text{II}}_2\text{Ti}^{\text{III}}_2$ clusters with a total spin $S_{\text{T}} = 4$ ($12.65 \mu_{\text{B}}$, $g = 2.00$). The magnetostructural correlation between the $\text{Mn}^{\text{II}}\text{–Cl–Mn}^{\text{II}}$ bond angle and the exchange constant $J_{\text{Mn–Mn}}$ is well-established.^{20,21} Magnetic interactions usually have an antiferromagnetic character, but there is a narrow angle interval ($93\text{–}98^\circ$) where the exchange is very weak or even ferromagnetic. The Mn–Cl–Mn bond angle in complex **8** is $97.08(5)^\circ$, and it is assumed that the Mn_4Ti_4 cluster may be treated as a Mn_2Ti_2 dimer containing only weakly interacting halves. The experimental data were fitted using the Kambe vector coupling method.²² The exact symmetry of the Mn_2Ti_2 cluster is low, but a reasonable simplifying

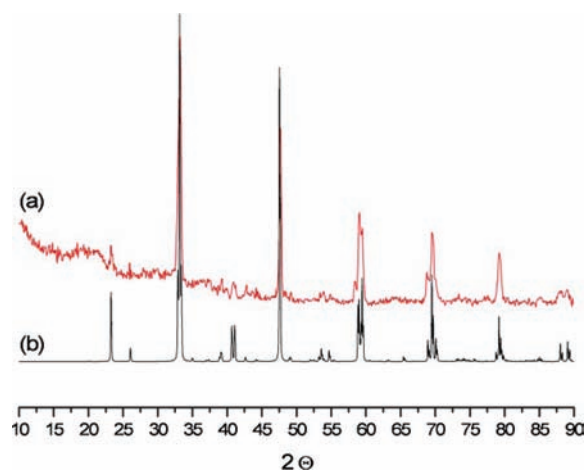


Figure 9. Powder XRD patterns: (a) precursor **6** decomposed at 1400°C in an air atmosphere, (b) CaTiO_3 (ICSD 16688).

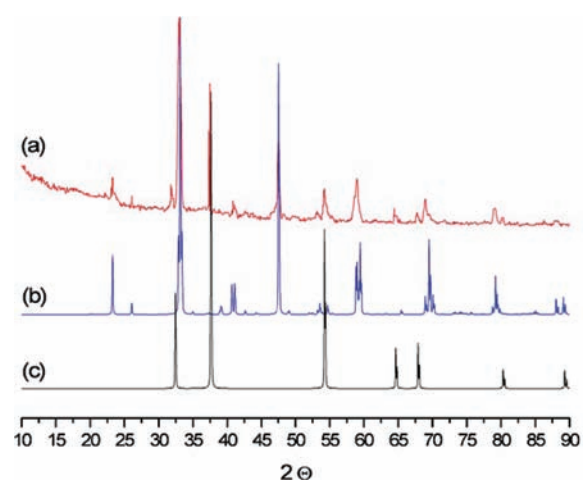


Figure 10. Powder XRD patterns: (a) precursor **7** decomposed at 1400°C in an air atmosphere, (b) CaTiO_3 (ICSD 16688), (c) CaO (ICSD 1922).

approximation is possible by neglecting $\text{Mn1}\cdots\text{Mn2}$ ($6.190(2)$ Å) and taking equal $\text{Mn1}\cdots\text{Ti1}$ ($3.706(2)$ Å) and $\text{Mn1}\cdots\text{Ti2}$ ($3.631(2)$ Å) as well as $\text{Mn2}\cdots\text{Ti1}$ ($3.315(2)$ Å) and $\text{Mn4}\cdots\text{Ti3}$ ($3.350(2)$ Å) magnetic interactions (Scheme 6).

The magnetization of complex **8** was calculated in a magnetic field of 500 mT using the method described by Belorizky.²³ Least-squares fitting of the data gave $J_{\text{Ti–Ti}} = -27.7 \text{ cm}^{-1}$, $J_{\text{Ti–Mn}} = -5.2 \text{ cm}^{-1}$, $g = 1.98$, and $zJ' = 0.017 \text{ cm}^{-1}$. Temperature-independent paramagnetism was set at $130 \times 10^{-6} \text{ emu mole}^{-1}$ for Ti(III) and 0 for Mn(II) ions.²⁴ No paramagnetic impurity was needed for the simulation. The agreement factor $R = \sum[(\chi T)_{\text{exp}} - (\chi T)_{\text{calcd}}]^2 / \sum[(\chi T)_{\text{exp}}]^2$ was 8.7×10^{-5} (68 points). The ground state was found to be $|S_{\text{T}}, S_{\text{Ti}}, S_{\text{Mn}}\rangle = |4, 1, 5\rangle$ ($S_{\text{Ti}} = S_{\text{Ti1}} + S_{\text{Ti2}}$, $S_{\text{Mn}} = S_{\text{Mn2}} + S_{\text{Mn4}}$, and $S_{\text{T}} = S_{\text{Ti}} + S_{\text{Mn}}$) with the 6-fold degenerate $|n, 0, n\rangle$ state ($n = 0\text{–}5$) at 7.3 cm^{-1} above the ground state. The fitting procedure as well as the calculation of field dependence of magne-

(18) Roubeau, O.; Clérac, R. *Eur. J. Inorg. Chem.* **2008**, 28, 4325–4342.

(19) (a) Sokol, J. J.; Hee, A. G.; Long, J. R. *J. Am. Chem. Soc.* **2002**, 124, 7656–7657. (b) Osa, S.; Kido, T.; Matsumoto, N.; Re, N.; Pochaba, A.; Mroziński, J. *J. Am. Chem. Soc.* **2004**, 126, 420–421. (c) Zaleski, C. M.; Depperman, E. C.; Kampf, J. W.; Kirk, M. L.; Pecoraro, V. L. *Angew. Chem., Int. Ed.* **2004**, 43, 3912–3914. (d) Mishra, A.; Wernsdorfer, W.; Abboud, K. A.; Christou, G. *J. Am. Chem. Soc.* **2004**, 126, 15648–15649. (e) Choi, H. J.; Sokol, J. J.; Long, J. R. *Inorg. Chem.* **2004**, 43, 1606–1608. (f) Oshio, H.; Nihei, M.; Yoshiola, A.; Nojiri, H.; Nakano, M.; Yamaguchi, A.; Karaki, Y.; Ishimoto, H. *Chem. Eur. J.* **2005**, 11, 843–848. (g) Aromí, G.; Brechin, E. K. *Struct. Bonding (Berlin)* **2006**, 122, 1–67.

(20) Martín, J. D.; Hess, R. F.; Boyle, P. D. *Inorg. Chem.* **2004**, 43, 3242–3247.

(21) Romero, I.; Rodríguez, M.; Llobet, A.; Corbella, M.; Fernández, G.; Collomb, M.-N. *Inorg. Chim. Acta* **2005**, 358, 4459–4465.

(22) Kambe, K. *J. Phys. Soc. Jpn.* **1950**, 15, 48–51.

(23) Belorizky, E.; Fries, P. H.; Gojon, E.; Latour, J.-M. *Mol. Phys.* **1987**, 61, 661–668.

(24) Sekutowski, D.; Jungst, R.; Stucky, G. D. *Inorg. Chem.* **1978**, 17, 1848–1855.

tization are described in detail in the Supporting Information.

Thermal Decomposition of 6 and 7. The heterobimetallic complexes **6** and **7** seem to be natural precursors for ceramic materials. They already have metal ratios typical for perovskite and spinel materials, respectively. These compounds were subjected to preliminary tests and thermally decomposed in atmospheric air. The resulting materials were analyzed by powder XRD analysis. The diffraction patterns were obtained for **6** and **7**, both thermolyzed at 1400 °C. The XRD pattern for compound **6** is an exact match to those for CaTiO₃ perovskite (Figure 9), and the PXRD spectrum of complex **7** can be assigned to a mixture of CaTiO₃ and CaO, while the decomposition pathway is typical of SSP-III,²⁵ where there are both double and mono-oxides (Figure 10).

Conclusions

In summary, we have developed a simple and efficient strategy for the synthesis of nonorganometallic, heterometallic clusters from cheap organometallic precursors. We believe that the new synthetic route will be easily generalized, making other as yet unknown heteropolymetallic compounds with other d- and f-block metallocenes accessible. In that case, we are sure that proper selection of the starting materials as well as reaction conditions can lead to the preparation of interesting objects with single-molecule magnetic properties. Complex **8** belongs to a group of magnetic clusters that consist of Mn₄ subunits held together by two μ -Cl bridges.²⁶ Although **8** is not a SMM, we believe that the

synthetic route may be of great interest to chemists involved with high-spin clusters, and more generally molecular magnetism. Furthermore, the resulting compounds **6** and **7** have a fixed metal ratio typical for perovskite and spinel materials. In the case of complex **7**, the expected spinel was not formed. This may be due to the presence of chlorine atoms in the compound.²⁵ In the literature, there are some known examples of heterobimetallic acetate chlorides, for instance, [Zn₇(OAc)₁₀(μ -OH)₆Cu₅(dmae)₄Cl₄] (where dmae = (N,N-dimethylamino)ethanolate), that have been used in chemical vapor deposition to give the double-oxide Cu₅Zn₇O₁₂.²⁷ A very attractive feature of species **1–9** is that the metal ions have terminal chloride ligands for substitution reactions to prepare larger molecules by a building-block approach. These findings provide a good illustration of the capabilities of the new synthetic method.

Acknowledgment. The authors would like to thank the Polish State Committee for Scientific Research Grants N205 4036 33 and the Foundation for Polish Science (START Programme for Young Scientists) for their support of this research.

Supporting Information Available: Full crystallographic data and molecular structures of **1–9**, ¹H NMR spectra for reaction of Cp₂TiCl₂ with CaL'₂ and L'H (molar ratio 1:2:6) in toluene-d₈, GC-MS data (CpH/Ti ratio versus time plot for Cp₂TiCl₂ reactions with metallic Ca and CaL₂), and a powder XRD spectrum for **9** decomposed at 950 °C are provided. This material is available free of charge via the Internet at <http://pubs.acs.org>.

(25) Veith, M. J. *J. Chem. Soc., Dalton Trans.* **2002**, 2405–2412.

(26) Yoo, J.; Wernsdorfer, W.; Yang, E.-C.; Nakano, M.; Rheingold, A. L.; Hendrickson, D. N. *Inorg. Chem.* **2005**, *44*, 3377–3379.

(27) Hamid, M.; Tahir, A. A.; Mazhar, M.; Zeller, M.; Hunter, A. D. *Inorg. Chem.* **2007**, *46*, 4120–4127.